


# Comparative Investigation between In Situ Laser Ablation Versus Bulk Sample (Solution Mode) Inductively Coupled Plasma Mass Spectrometry (ICP-MS) Analysis of Trinitite Post-Detonation Materials

Megan K. Dustin<sup>1</sup>, Elizabeth C. Koeman<sup>1</sup>, Antonio Simonetti<sup>1</sup>, Zachary Torrano<sup>1</sup>, and Peter C. Burns<sup>1,2</sup>

Applied Spectroscopy  
2016, Vol. 70(9) 1446–1455  
© The Author(s) 2016  
Reprints and permissions:  
sagepub.co.uk/journalsPermissions.nav  
DOI: 10.1177/0003702816662597  
asp.sagepub.com  


## Abstract

In the event of the interception of illicit nuclear materials or detonation of a nuclear device, timely and accurate deciphering of the chemical and isotopic composition of pertinent samples is pivotal in enhancing both nuclear security and source attribution. This study reports the results from a first time (to our knowledge), detailed comparative investigation conducted of Trinitite post-detonation materials using both solution mode (SM) and laser ablation (LA) inductively coupled plasma mass spectrometry (ICP-MS) techniques. Trace element abundances determined for bulk Trinitite samples subsequent to digestion and preparation for SM-ICP-MS analysis compare favorably to calculated median concentrations based on LA-ICP-MS analyses for the identical samples. The trace element concentrations obtained by individual LA-ICP-MS analyses indicate a large scatter compared to the corresponding bulk sample SM-ICP-MS results for the same sample; this feature can be attributed to the incorporation into the blast melt of specific, precursor accessory minerals (minerals in small quantities, such as carbonates, sulfates, chlorites, clay, and mafic minerals) present at ground zero. The favorable comparison reported here validates and confirms the use of the LA-ICP-MS technique in obtaining accurate forensic information at high spatial resolution in nuclear materials for source attribution purposes. This investigation also reports device-like  $^{240}\text{Pu}/^{239}\text{Pu}$  ratios ( $\sim 0.022$ ) for Pu-rich regions of the blast melt that are also characterized by higher Ca and U contents, which is consistent with results from previous studies.

## Keywords

Trinitite, post-detonation material, inductively coupled plasma mass spectrometry, laser ablation, nuclear forensics

Date received: 7 April 2015; revised: 23 December 2015; accepted: 8 March 2016

## Introduction

Post-detonation nuclear forensics, a burgeoning research field, was born out of necessity in the modern age of nuclear weapons production. The ability to identify the perpetrators of a nuclear strike is paramount to national security, both in the event of an attack and to deter nations, terrorist organizations, or individuals from aggression for fear of attribution.<sup>1</sup> At present, the majority of nuclear forensic research is conducted within the auspices of government national laboratories, which have access to “classified” nuclear materials, such as those originating from underground nuclear test sites. As such, a significant portion of the results obtained at United States of America

national laboratories are not reported in the public domain, and therefore awareness to the expertise in this field is somewhat hindered, i.e., any new developments in

<sup>1</sup>Department of Civil and Environmental Engineering and Earth Sciences, University of Notre Dame, USA

<sup>2</sup>Department of Chemistry and Biochemistry, University of Notre Dame, USA

### Corresponding author:

Elizabeth C. Koeman, Department of Civil and Environmental Engineering and Earth Sciences, University of Notre Dame, Notre Dame, IN 46556, USA.

Email: elizabethkoeman@gmail.com

protocols or analytical methods are not easily conveyed to researchers at academic institutions.

In contrast, the location and occurrence of the first atomic bomb test, the Trinity site, provides declassified post-detonation materials (PDMs) for nuclear forensic investigations.<sup>2–5</sup> Studying the remnant blast material from the Trinity site, referred to as Trinitite, is extremely useful because information relative to both the construction and device components of the Trinity bomb is available in the public domain.<sup>2</sup> Therefore, chemical (major and trace element) and isotopic (U, Pu) results obtained from Trinitite can be compared to the known compositions of the bomb and the natural geological background.<sup>5–9</sup>

The Trinity nuclear test occurred on the morning of 16 July 1945 at the White Sands Proving Ground in New Mexico. The bomb was detonated from atop a 30 m steel blast tower, and the ensuing mushroom cloud was recorded to reach a height of 15.2–21.3 km and a temperature of >8000 K.<sup>3</sup> The Trinitite material formed subsequent to the detonation was a result of fusion of the arkosic desert sand (i.e., natural geological background), and bomb and ground zero (GZ) site components due to the extremely elevated temperature and shock wave. A two-step formational process has been hypothesized for the creation of Trinitite: melting and fusion of material, and subsequent raining down of airborne, solid particles (including blast melt) from the mushroom cloud that were subsequently incorporated into the surface of Trinitite.<sup>10</sup> Because the temperature and radiation levels were likely higher for Trinitite formed closer to GZ, the latter should in theory display a greater degree of mixing (of bomb and natural components) from increased melting, as well as higher concentrations of radioactive Pu and U (the latter from the tamper) contained within the nuclear device.<sup>3</sup> Conversely, Trinitite collected farther from ground zero should have experienced less mixing and therefore contain a greater number of inclusions due to preferential fallout of metals at the periphery of the mushroom cloud.<sup>3</sup>

The geologic composition of the area at GZ is dominantly arkosic sand and dominated by quartz and feldspars (plagioclase and K-feldspar), but also includes accessory minerals such as carbonates, sulfates, chlorites, clay, and mafic minerals.<sup>1–3</sup> Bomb components include Pu fuel from the core, U and Pb from the tamper, Cu from the wiring, Fe and Ti from the blast tower, as well as other trace metals (e.g., Nb and Ta), and does not contain any other trace element analyzed here in any appreciable quantity.<sup>2,8,9</sup> The resulting Trinitite material is extremely heterogeneous and consists of a “glassy” (top) and a “sandy” (bottom) side, with the former corresponding to the desert surface that was most exposed to heat and radiation from the blast (see Figure S1 in the Supplemental Material online).

Because of Trinitite’s inherent heterogeneous nature (see Figure 1), several previous studies have primarily utilized a laser ablation inductively coupled mass spectrometry

(LA-ICP-MS) approach in order to document chemical and isotopic results at high spatial resolution (i.e., tens of micron scale).<sup>5–7,9,11</sup> In order to test the validity of this approach, this study processed bulk Trinitite samples by sample digestion and subsequent analysis by solution mode (SM)-ICP-MS. In addition, in order to conduct a valid comparison between solution (bulk) and LA modes of analyses, individual LA measurements were compiled so as to generate median elemental abundance values for each individual Trinitite sample; this data treatment helped to better discern chemical and isotopic trends. Ultimately, this comparative study will also permit a better understanding of Trinitite’s complex chemical and isotopic nature.

## Analytical methods

### Samples

Trinitite samples investigated here were purchased from the Mineralogical Research Corporation ([www.minresco.com](http://www.minresco.com)). Samples analyzed by LA-ICP-MS were cut and polished into thin sections ranging in thickness from 60–100  $\mu\text{m}$ . Most thin section samples of Trinitite exhibit a melt glass top layer transitioning into a sandy base (Figure S1).<sup>11</sup> Based on alpha track radiography patterns, however, several samples (e.g., sample I 7.76 c)<sup>7</sup> investigated here appear to consist entirely of melt glass, and therefore most likely represent a “non-vertical” slice. To validate the results obtained for our comparative study, aliquots of samples used for SM analyses were prepared from sections of bulk samples that had previously been cut and polished for thin section production and subsequently analyzed by LA-ICP-MS. Unfortunately, the spatial (geographic) distribution of the Trinitite samples relative to ground zero is not available due to bulldozing of the site in the 1950s. However, relative distances were calculated by measuring the <sup>152</sup>Eu activity by gamma spectroscopy, and these correspond to calculated distances that range between 41 and 74 m from ground zero;<sup>12</sup> sample TS3 records the highest <sup>152</sup>Eu activity and therefore yields the closest calculated distance (41 m). Several samples of Trinitite lacked <sup>152</sup>Eu activity and are therefore classified as having formed at >74 m. Calculated distances for all samples investigated here are listed in Table S1.

### Laser ablation inductively coupled mass spectrometry

In order to determine optimal locations for LA-ICP-MS spot analyses, samples were first examined by alpha-track radiography and scanning electron microscopy (SEM). For alpha-track radiography, samples were placed atop CR-39 plastic detectors for 10 days and subsequently etched with 6.25 M NaOH at 98 °C. This process reveals the locations of the highest concentrations of alpha-emitters (primarily U and Pu), since these particles mark the plastic over the

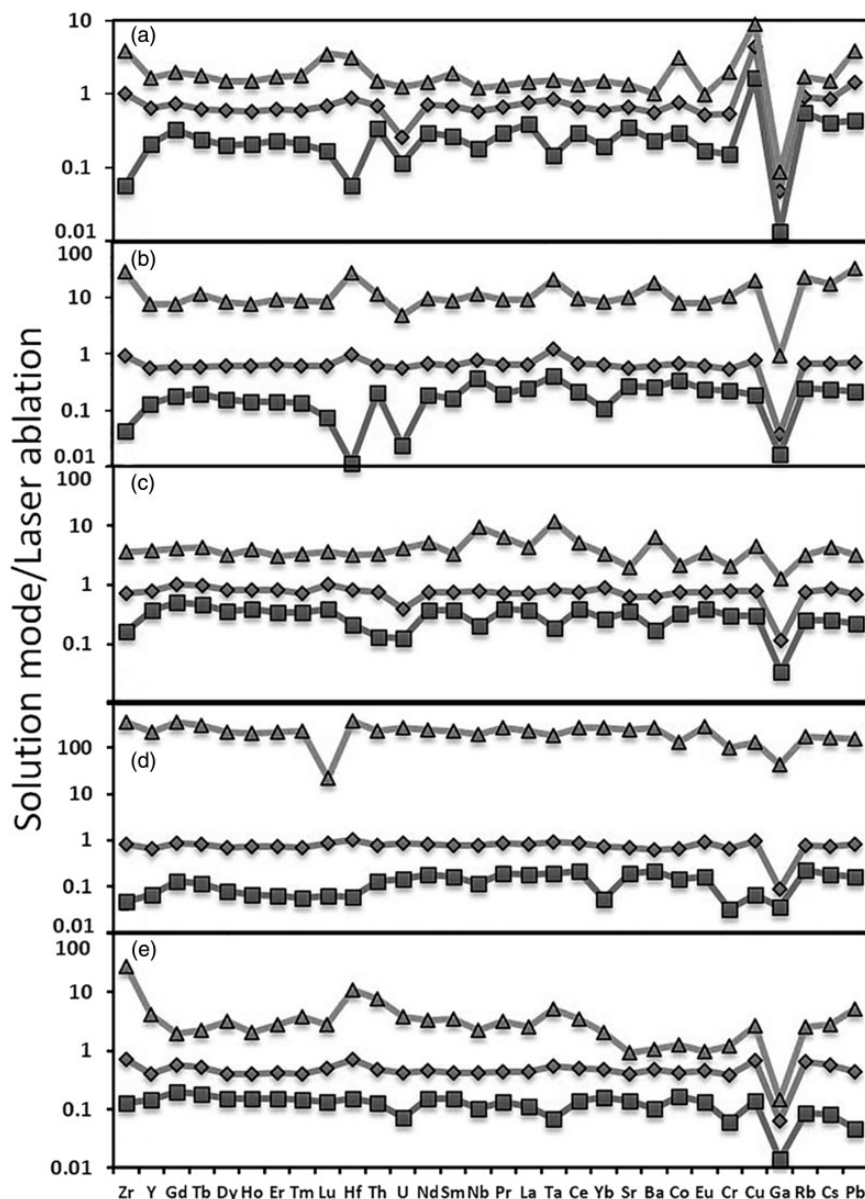


**Figure 1.** SM-ICP-MS results compared with LA analyses from the same Trinitite samples: (a) 4C 10.60a; (b) 1 7.76c; (c) 4B 11.59a; (d) 5B 10.22b; and (e) 3 5.25b. Triangles correspond to “minimum”, diamonds to “median”, and squares to “maximum”.

course of 10 days. Images of the alpha-tracks were taken under plane-polarized light with a petrographic microscope equipped with a digital camera and colored red using Adobe Photoshop. These images were then overlain by plane-polarized light images of the thin sections. Back scatter electron (BSE) images were also collected using an EVO 50 LEO SEM located at the Notre Dame Integrated Imaging Facility in order to investigate the major element compositions of the Trinitite samples investigated here. An accelerating voltage of 20 kV and magnification of 100–200 $\times$  were utilized for these images. For example, areas characterized by an average low mass number consist largely of Si, which is an element derived predominantly from quartz present within the desert sand (geological

background) at GZ, and therefore these regions are not of significant interest for nuclear forensic purposes. The main reason being that Wallace et al. clearly show that quartz-rich areas of Trinitite are devoid of bomb-related chemical constituents.<sup>7</sup>

Electron microprobe analyses (EMPA) were conducted at the University of Chicago using a Cameca SX-50 electron microprobe with a 15  $\mu\text{m}$  spot size. Electron microprobe data were needed in order to have an internal standard (i.e., CaO wt % abundances) for LA work subsequently conducted on a ThermoFinnegan Element2 High-Resolution (HR)-ICP-MS instrument coupled to a New Wave Research UP-213 laser system. Spots were chosen to be representative of blast melt areas for all samples

while avoiding Si-rich regions (i.e., >60 wt % for the reasons stated earlier), and focusing on areas that record high concentrations of alpha particles and high atomic mass (in BSE-SEM images). Abundances of CaO wt % were determined for each individual LA area. Parameters used for LA analysis were power level of 100% (corresponding fluence of  $\sim 10\text{--}12\text{ J/cm}^2$ ), spot size of 45  $\mu\text{m}$ , and a repetition rate of 5 Hz. Approximately 300 laser shots were fired for each LA location. A standard-sample bracketing technique was used employing the NIST SRM 612 glass wafer as an external standard to monitor instrumental drift and for determination of trace element abundances. All elemental abundances (ppm) were calculated using the Glitter LA data reduction software.<sup>13</sup> Since Pu is not present in the NIST SRM 612 standard, the absolute abundances of Pu were not determined; however, background-subtracted <sup>239,240</sup>Pu ion signals (counts per second, or cps) are used as a proxy for the concentrations of Pu within the samples investigated here. The relative uncertainties associated with each individual LA analysis are not listed in Table S3 since this would result in reporting an extremely large data table. Table S3 lists both the calculated mean and median elemental abundances obtained by LA-ICP-MS analyses. However, the relative uncertainties or internal precision (as calculated by the Glitter data reduction software) vary according to the determined elemental abundances (i.e., function of ion signal size and consequently influencing counting statistics), and can be effectively summarized in the following manner: for reported concentration >100 ppm, the associated relative uncertainty is between  $\sim 2$  and  $\sim 5\%$  ( $2\sigma$ ); for determined elemental abundances between 10 and 100 ppm, the associated uncertainty varies between  $\sim 5$  and  $\sim 10\%$  ( $2\sigma$ ); and for concentrations <10 ppm, the relative uncertainties range between  $\sim 10$  and  $\sim 20\%$  ( $2\sigma$ ). Of importance, the relative uncertainties associated with the LA-ICP-MS analyses reported here (in terms of absolute abundances) are insignificant when compared to the total range in elemental concentrations determined by LA-ICP-MS analyses (see Figures 1, 2 and S2), and therefore do not alter the observations and interpretations presented in the subsequent sections of this paper.

### *Solution mode inductively coupled mass spectrometry*

Prior to SM-ICP-MS analyses, bulk Trinitite samples were crushed into a fine powder using an agate mortar and pestle, and an aliquot of sample powder ( $\sim 0.050\text{ g}$ ) was placed in a solution containing double-distilled (2D), concentrated HNO<sub>3</sub> acid and 2D concentrated HF acid (1:4 ratio mixture) within a pre-cleaned 15 mL Savillex Teflon beaker. The bulk sample digestion procedure followed the method outlined by Bellucci et al.<sup>8</sup> Sample solutions were then prepared for SM-ICP-MS analysis using a standard/spike addition method.<sup>14</sup> All SM analyses were conducted

on the same ThermoFinnigan Element2 HR-ICP-MS instrument used for the LA analyses.

## **Results**

### *Solution mode ICP-MS analyses*

Solution mode ICP-MS elemental abundance data obtained for bulk Trinitite samples are listed in Table S2 and are compared to those obtained by LA for the same samples (Table S3; Figure 1), and unmelted bulk sand (US) values collected from the bottom of Trinitite determined by SM-ICP-MS (Figure 2).<sup>8</sup> In Figures 1 and 2, elements are listed according to their respective condensation temperatures (decreasing order). Figure 1 illustrates three patterns that are labeled minimum, maximum, and median, which correspond to the individual LA analyses that record the lowest, highest, and calculated median elemental abundances, respectively. Therefore, the minimum pattern will always display the highest ratios when compared to the elemental concentrations obtained for the bulk sample SM analyses (Figure 1); the inverse result applies when the bulk sample is compared to the LA analysis yielding the highest trace element abundances, i.e., the maximum curve will always yield the lowest ratios. This comparison between the bulk sample result obtained in SM and LA analyses permits evaluation of the micron-scale chemical heterogeneity of Trinitite; hence sample I 7.76c exhibits greater heterogeneity compared to sample 4B 11.59a (Figure 1) because there is a greater spread between the curves labeled maximum and minimum. Of importance, the comparative values/ratios obtained for the calculated median LA concentrations are very close to unity (i.e., value of 1) for most elements for all samples, in particular for samples 4B 11.59a and 5B 10.22b (Figure 1c and d). A majority of the median values are slightly below a value of 1 and can be attributed to the dilution effect for elemental concentrations determined for the SM analyses, which included the digestion of quartz and/or quartz-rich blast melt. It has been documented in earlier studies that quartz-rich regions of Trinitite are essentially devoid of trace elements.<sup>7</sup> As stated earlier, quartz-rich regions of Trinitite were purposely avoided during LA analyses.

Of interest, the maximum and minimum normalized values exhibited in Figure 1 do not necessarily record similar negative or positive elemental anomalies, which once again attest to the extremely heterogeneous nature of Trinitite at the micron scale.<sup>7–11</sup> For example, in Figure 1b the maximum pattern for sample I 7.76c indicates large negative anomalies for Hf, Zr, and U, which may be attributed to the analysis of zircon-rich blast melt during LA analysis. Bellucci et al. emphasize the importance of the incorporation of precursor accessory minerals such as zircon, monazite, and apatite in controlling the trace element signature of Trinitite blast melt.<sup>8</sup> Similar negative

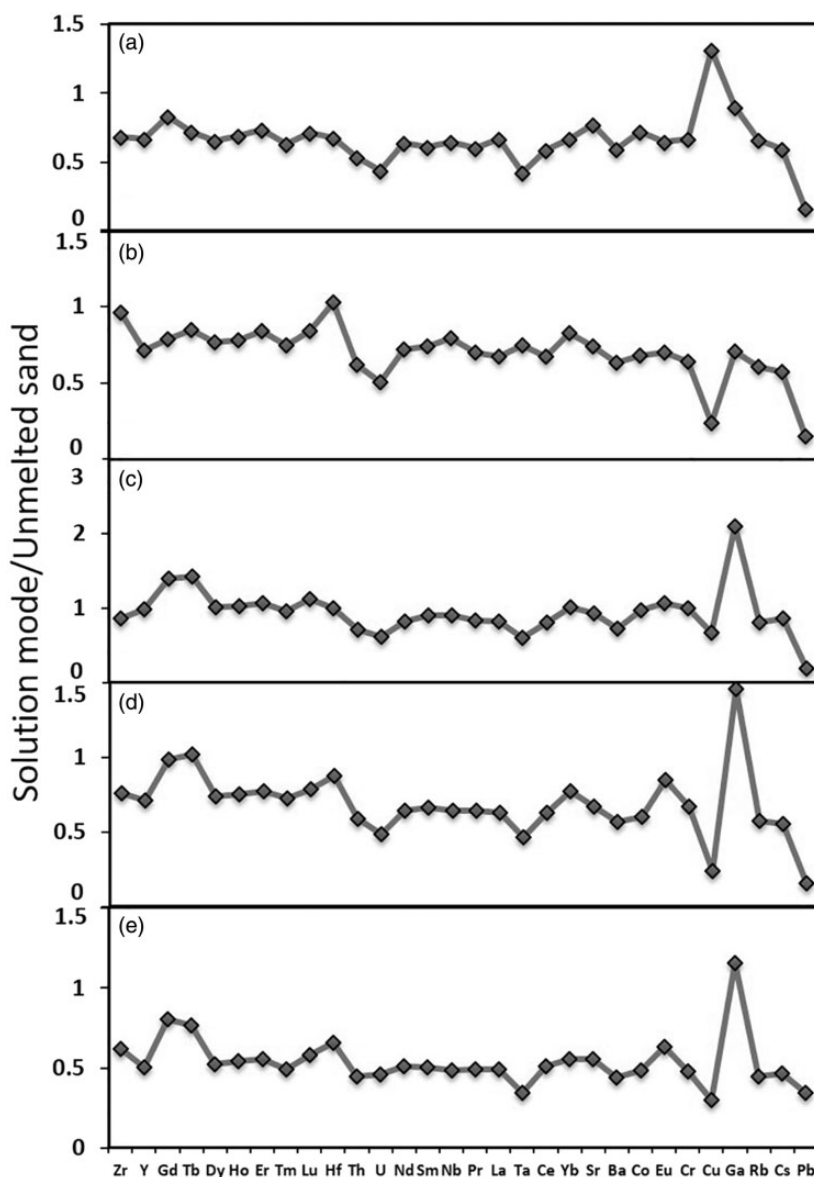


**Figure 2.** SM-ICP-MS elemental abundances determined for samples (a) 4C 10.60a, (b) 1 7.76c, (c) 4B 11.59a, (d) 5B 10.22b, and (e) 3 5.25b compared to corresponding concentrations for unmelted arkosic sand (US; from Bellucci et al.<sup>8</sup>).

anomalies are shown for these same elements for samples 4B 11.59a and 4C 10.60a, but are not as pronounced. Positive elemental anomalies for Ta, Nb, Ba, Cu, and Pb seen in the minimum curves for samples in Figure 1 can be attributed to the presence of bomb-related, anthropogenic chemical components.<sup>9,10</sup> Moreover, the large negative Ga anomalies shown in Figure 2 for all of the patterns is related to an isobaric spectral interference produced during the LA analyses that artificially augments the calculated concentrations of Ga; this feature is examined in greater detail in the discussion section below. Figure 2 compares the elemental abundances obtained for the bulk sample SM analyses for the same samples versus the corresponding elemental concentrations for the unmelted US bulk sand at

ground zero.<sup>8</sup> Overall, the concentrations obtained for the SM analyses for a majority of the elements are similar to those for the US since the comparative values are close to unity (Figure 2); however, notable negative anomalies are recorded in these samples for both Cu and Pb (Figure 2). Interestingly, only sample 4C 10.60a shows a positive Cu anomaly rather than a negative one, indicating it may have incorporated more bomb-related Cu. Three of the samples (Figure 2c, d, and e) show positive Ga anomalies, although their corresponding LA comparative plots (Figure 1) still show significantly lower Ga values for LA analyses compared to SM.

The rare earth element (REE) abundances obtained for the LA analyses (median values), SM results (bulk sample)

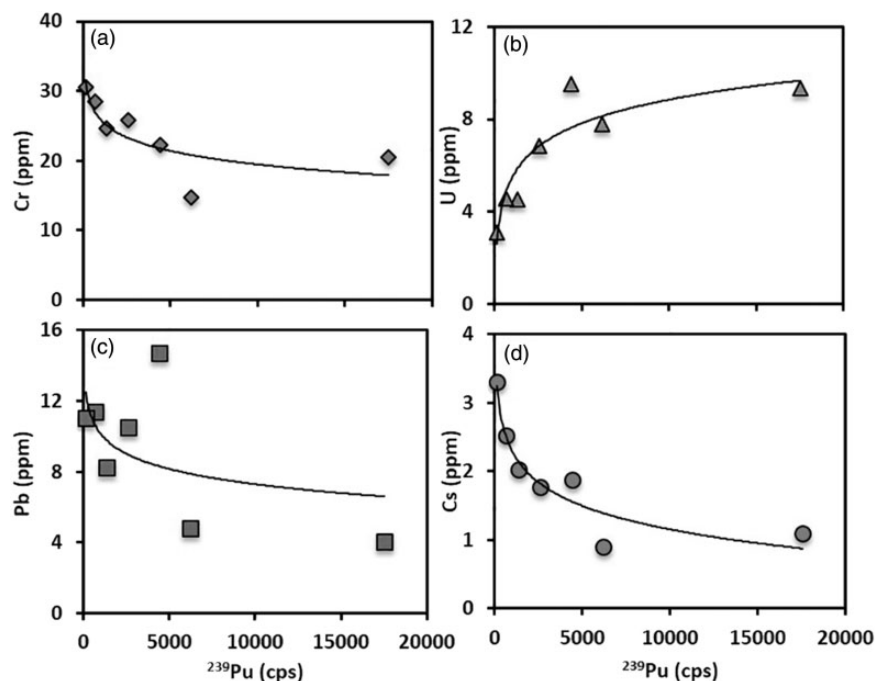


**Figure 3.** Plots illustrating the median elemental abundances of Cr, U, Pb, and Cs vs.  $^{239}\text{Pu}$  ion signal (cps): (a) Cr vs.  $^{239}\text{Pu}$ ; (b) U vs.  $^{239}\text{Pu}$ ; (c) Pb vs.  $^{239}\text{Pu}$ ; (d) Cs vs.  $^{239}\text{Pu}$ .

(Tables S1 and S2), and US are shown as chondrite normalized values in Supplementary figure S2;<sup>8</sup> normalizing the REE abundances to chondrite concentrations allows for easier comparison of elemental variations as this eliminates the Oddo–Harkins effect. The patterns demonstrate that the REE signatures for the SM, LA, and US analyses are essentially identical. In general, the LA results yield the highest REE concentrations, followed by US and then SM.

### Laser ablation ICP-MS analyses

In general, the median values calculated for major element abundances reported here for Trinitite obtained by EMPA are comparable to those for average arkosic sand (Figure S3 and Table S3).<sup>15</sup> However, the Trinitite samples investigated here display lower  $\text{SiO}_2$  and higher CaO wt% abundances, which typically range between 70 and 85 wt%  $\text{SiO}_2$  and <3 wt% CaO in natural arkosic sands.<sup>12</sup> The lower abundances of  $\text{SiO}_2$  reported here may be due to the tendency to avoid relict quartz grains during LA-ICP-MS analysis, which are purposely omitted for forensic analysis as these originate from the geological background, and hence do not host any bomb-related components. The enrichment in CaO wt% can be explained by local gypsum deposits, which impart a calcareous signature to the sand deposits within the Trinity area.<sup>8</sup> On the basis of the data shown in Figure S3, there are significant negative correlations between  $\text{K}_2\text{O}$  and  $\text{SiO}_2$  wt

% abundances and the  $^{239}\text{Pu}$  ion signal; in contrast to the major elements, the presence of  $^{239}\text{Pu}$  is derived entirely from the nuclear device. The inverse relationship between Pu (ion signal is a proxy for concentration) and Si abundances corroborates the same finding as reported by Wallace et al.<sup>7</sup> In contrast, general positive trends are noted between the  $^{239}\text{Pu}$  ion signal and median FeO and MnO concentrations (Supplemental figure S3c and f), while  $\text{Na}_2\text{O}$  concentration does not show any systematic variation with Pu.

Figure 3 illustrates the variation between the median abundances of bomb-related chemical components (Cr, Pb, U) and the  $^{239}\text{Pu}$  ion signal measured during LA analyses. Three of the elements (Cr, Pb, and Cs) define general negative logarithmic curves against  $^{239}\text{Pu}$  ion signals, whereas U defines a relatively positive logarithmic relationship (Figure 3). The concentrations of Pb, Cs, and U (Figure 3) within most samples of Trinitite are similar to those of average continental crust,<sup>16</sup> although several display enrichments in Pb, Ta, and Rb, and depletions in Co (>1.5 ppm Co in sand/continental crust; Table S3).<sup>6</sup>

On the basis of elemental melt temperatures, Bellucci et al. proposed that the peripheral zone of the Trinity blast site contains higher concentrations of elements or metals characterized by lower melting temperatures (i.e., more volatile),<sup>8</sup> such as Cu and Pb and contain a higher amount of inclusions due to preferential fallout. Conversely, samples that originate closer to ground zero will tend to show fewer inclusions, stronger alpha

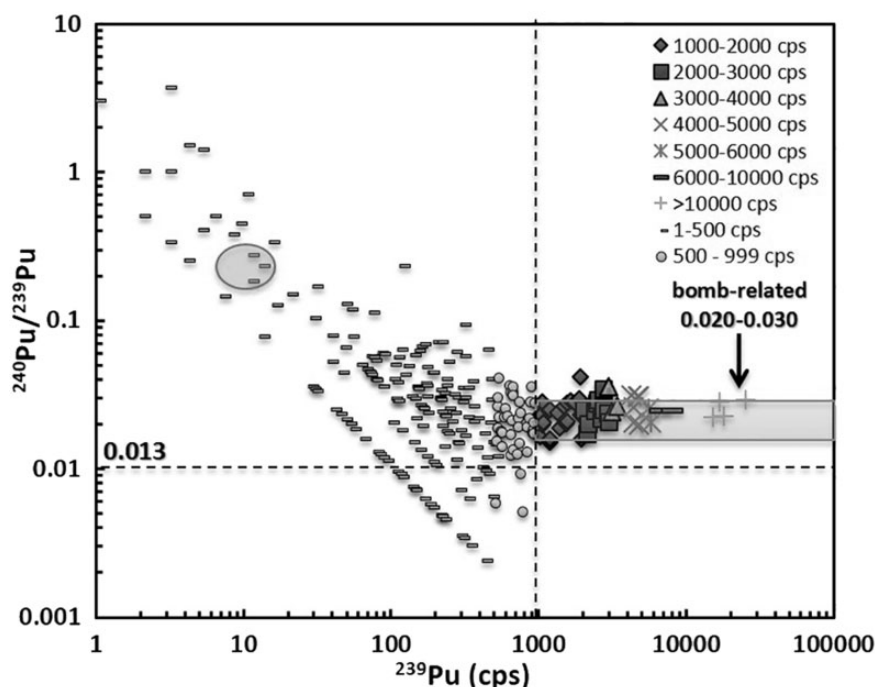


**Figure 4.** Diagram illustrating the compilation of  $^{240}\text{Pu}/^{239}\text{Pu}$  ratio vs.  $^{239}\text{Pu}$  ion signal from laser ablation analyses of several samples ( $n=9$ ) of Trinitite. Ablations are grouped according to their  $^{239}\text{Pu}$  ion signal intensities. A value of 0.013 represents the calculated  $^{240}\text{Pu}/^{239}\text{Pu}$  composition of the Trinity device,<sup>2</sup> and the range of background  $^{240}\text{Pu}/^{239}\text{Pu}$  ratios, from fallout due to atmospheric testing,<sup>17</sup> is highlighted with a circle. Ablation spots that yield a bomb-related signature ( $^{240}\text{Pu}/^{239}\text{Pu}$  of 0.020–0.030 and  $^{239}\text{Pu}$  of  $>1000$  cps) are also highlighted.

emission track patterns, record higher Pu ion signals during LA-ICP-MS analysis, and bomb-like (supergrade)  $^{240}\text{Pu}/^{239}\text{Pu}$  ratios. Initial synthesis of the entire LA data set, in particular for  $^{240}\text{Pu}/^{239}\text{Pu}$  ratios, was conducted on the basis of each individual analysis. This strategy, however, produced a chaotic “picture” that resulted in no discernable trends. Thus, in order to simplify the comparisons of the LA results to those for the bulk Trinitite analyses obtained by SM-ICP-MS, individual LA data points were grouped arbitrarily according to the strength of their corresponding  $^{239}\text{Pu}$  ion signals (cps). The groups are: 1–500, 500–999, 1000–2000, 2000–3000, 3000–4000, 4000–5000, 5000–6000, 6000–10 000, and  $>10\ 000$  (see Supplementary table S4). Median values were then calculated for each of these groupings, and consequently LA analyses that yielded  $>1000$  cps  $^{239}\text{Pu}$  recorded the lowest  $^{240}\text{Pu}/^{239}\text{Pu}$  ratios of between 0.020 and 0.030 (Figure 4; Supplementary table S4). These values are higher than the calculated  $^{240}\text{Pu}/^{239}\text{Pu}$  ratio of 0.0132 for the Trinity device,<sup>2</sup> but overlap the Pu isotope ratios reported for bulk analyses of Trinitite from previous studies,<sup>6,7</sup> and are significantly lower than the natural fallout (background)  $^{240}\text{Pu}/^{239}\text{Pu}$  ratio of 0.176 for the Trinity site.<sup>17</sup> Finally,  $^{240}\text{Pu}/^{239}\text{Pu}$  ratios for ablation runs recording  $<1000$  cps for the  $^{239}\text{Pu}$  ion signal are generally higher (vary between 0.030 and 0.230; Figure 4).

## Discussion

### Comparison between LA- versus SM-ICP-MS Analyses

Overall, very good agreement exists between LA- and SM-ICP-MS analyses of Trinitite since the comparative factors (SM/LA) are very close to unity for most elements (Figures 1, 2, and S2). Thus, this result supports the utilization and validation of the LA-ICP-MS technique as a reliable tool for forensic analysis of complex post-detonation materials. However, there are some significant discrepancies between the concentrations determined by SM- versus LA-ICP-MS modes. For example, the significant negative Ga anomaly (e.g., Figure 1) recorded in all investigated samples may be attributed to a polyatomic spectral interference, which must occur solely during LA analysis as the comparative values are  $<1$ . During LA of Si-rich samples such as Trinitite, the possibility exists that  $^{29}\text{Si}$  combines with  $^{40}\text{Ar}$  in the plasma so as to produce an interference at mass 69 (equivalent in mass to  $^{69}\text{Ga}$ ). Cu anomalies, however, ranged from positive in sample 4C 10.60a to highly negative in sample 5B 10.22b. Thus, the distribution of Cu, which is believed to be bomb-related and originates from the copper wiring within the device, is extremely heterogeneous within Trinitite.<sup>3,8–10</sup> Overall, the SM/LA plots shown in Figure 1 display similar features, with all samples recording negative Ga anomalies (as explained above) but conflicting

anomalies for several elements, especially Zr and Hf. Hafnium is an element that originates predominantly from the geological background and is hosted primarily in accessory zircon found in the sand.<sup>8</sup> Therefore, the variable Hf-normalized values may simply be a function of the different amount of residual zircon that is either analyzed in situ within the blast melt and/or processed in the bulk Trinitite sample. Hence, the large discrepancy in the concentrations of trace elements controlled primarily by accessory mineral phases (e.g., Hf, Zr, U, and Th) between and within samples is simply a function of the previously noted, extensive heterogeneity of Trinitite. The REE chondrite normalized plots (Figure S2) show similar patterns between US and Trinitite samples, indicating that the device did not contain a significant amount of REEs. In all plots, the SM data plot below the corresponding LA and US chondrite normalized values. This feature can be attributed to a dilution effect, as the SM analysis represents digestion of bulk Trinitite containing quartz, which is essentially devoid of REEs. As a result, SM concentration data plots below the abundances obtained by LA while maintaining similar chondrite normalized REE patterns (Figure S2).

While SM-ICP-MS has proven here to be a useful tool for determining average values and establishing patterns for bulk Trinitite signatures, the material's high degree of chemical and mineralogical heterogeneity consequently results in LA analyses that reveal micron-scale details; e.g., the previously discussed Pu distribution and potential association with Ca,<sup>7</sup> which is further elaborated below. In light of the chaotic message provided when considering all LA data points (which vary greatly) independently, and the much more apparent trends/correlations after calculating and considering median values, it is imperative to conduct a significant number of LA analyses so as to generate a meaningful data set. However, the latter can be obtained

at a rapid rate (i.e., ~2 min per analysis), and therefore is still a time-effective strategy given the significant amount of time required to process bulk samples for SM-ICP-MS analysis (the latter requires a week or so to prepare including sample digestion). However, the spot size must be kept small enough to sample a relatively homogeneous area, such as the 45  $\mu\text{m}$  used for the analyses conducted here. Averaging LA-ICP-MS results for a large data set allows the chemical composition of bulk material to be assessed (quickly) while maintaining spatial resolution.

### Distribution of Pu

The heterogeneous nature of Trinitite, in particular the inhomogeneous distribution of Pu at the micron scale was investigated in greater detail. For example, due to the relative proximity of several LA spots (within tens of microns) for sample TSI with vastly different Pu contents (as recorded by highly variable  $^{239}\text{Pu}$  ion signals), it is unlikely that this significant difference is due to random incorporation. Hence, micro-X-ray fluorescence ( $\mu\text{-XRF}$ ) was utilized in order to further investigate the distribution of Pu in relation to the sample's major element composition. The results reveal that spot 12 (4412 cps;  $^{239}\text{Pu}$ ) lies within a Ca-rich area, whereas spot 11 (32 cps;  $^{239}\text{Pu}$ ) falls just outside the zone of Ca enrichment (Figure 5). The Ca-rich area may be attributed to the melting of relict calcite or gypsum that was incorporated into the Trinitite blast melt. An additional nine LA-ICP-MS analyses were performed in the zone of Ca enrichment, as well as in the surrounding areas and within more typical Trinitite glass (Figure 5).

The number of ablations performed was dependent on the availability of fresh glass devoid of vesicles (i.e., open

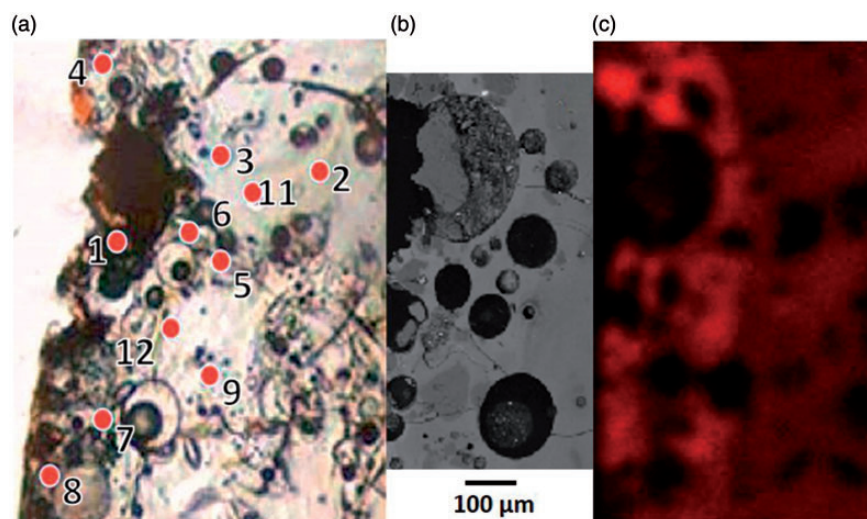


**Figure 5.** Area of interest within Trinitite sample TSI in relation to the distribution of Ca and Pu abundances, with locations of ablation spots marked by red circles: (a) plane polarized image; (b) back scatter electron picture; (c) micro-XRF map depicting the relative distribution of Ca abundances, brighter red areas are enriched in Ca.



spaces). Four of these additional analyses also yielded elevated  $^{239}\text{Pu}$  ion signals. Moreover, for ablations yielding  $>1000$  cps of  $^{239}\text{Pu}$  ion signal, a general linear positive trend with the  $^{43}\text{Ca}$  ion intensities is observed (Figure 6a). These same spots yield  $^{240}\text{Pu}/^{239}\text{Pu}$  ratios  $\sim 0.022$  (Figure 6b), which are distinct from the bulk glass surrounding the zone of enrichment. The correlation between Ca and Pu abundances (ion signals) in sample TSI (Figure 6) corroborates a similar result reported by Wallace et al.<sup>7</sup> Plotting the  $^{240}\text{Pu}/^{239}\text{Pu}$  ratio against  $^{239}\text{Pu}$  signal reveals that those ablations recording  $>1000$  cps have a distinct  $^{240}\text{Pu}/^{239}\text{Pu}$  ratio suggesting a definite bomb-related Pu signature (Figure 4). A negative correlation exists between  $^{240}\text{Pu}/^{239}\text{Pu}$  and  $^{239}\text{Pu}$  for ion signals  $<1000$  cps (counts

per second). In particular, there is a linear lower limit of  $^{240}\text{Pu}/^{239}\text{Pu}$  for samples with  $<1000$  cps. The counting statistics for the measurement of extremely low  $^{240}\text{Pu}$  ion signals renders the calculated  $^{240}\text{Pu}/^{239}\text{Pu}$  ratios for such analyses essentially invalid. Therefore, caution must be taken when interpreting the Pu isotope ratios as a function of measured ion signals. For example, the increasing  $^{240}\text{Pu}/^{239}\text{Pu}$  ratio with decreasing count rates (Figure 4) is not attributable to mixing between the bomb-device and "natural background".<sup>17</sup> The "natural  $^{240}\text{Pu}/^{239}\text{Pu}$  ratio" of 0.176 within the region of Alamogordo, New Mexico, represents the atom ratio for global fallout as a result of two decades of nuclear testing,<sup>17</sup> which had not yet occurred before the Trinity test. It has also been demonstrated that

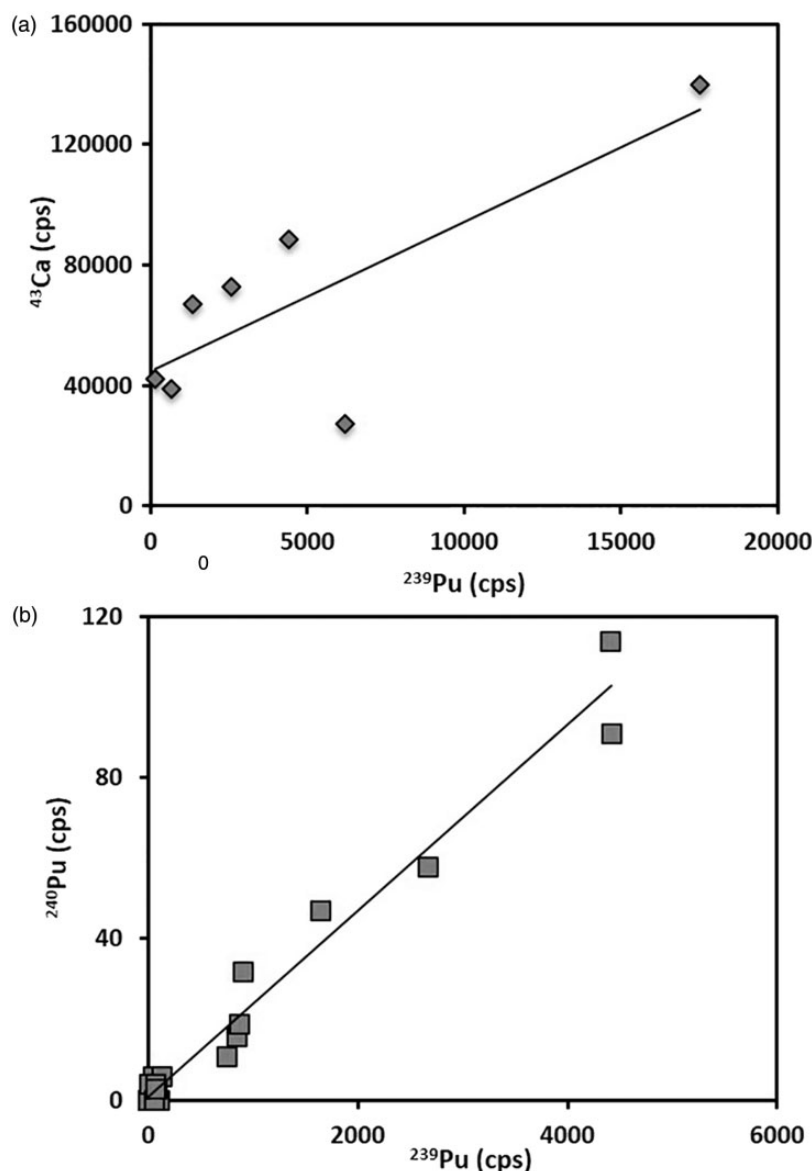


**Figure 6.** (a) Diagram of median ion signals for  $^{239}\text{Pu}$  vs.  $^{43}\text{Ca}$ ; and (b) plot of ion signals of  $^{239}\text{Pu}$  versus  $^{240}\text{Pu}$  for sample TSI. The analyses in (b) yield a constant and bomb-like  $^{240}\text{Pu}/^{239}\text{Pu}$  ratio = 0.022;  $R^2 = 0.94$ .

vitrification and the arid environment at the Trinity site has resulted in no observable leaching of radioactive components into the surrounding environment.<sup>3</sup> An alternative explanation is that natural fallout and bomb-related Pu may have mixed during petrographic thin section preparation of the Trinitite samples as water was used in their fabrication. However, the validity of this interpretation needs to be further investigated.

## Conclusions

This study reports for the first time a detailed comparison between elemental abundances obtained for bulk Trinitite samples measured by SM-ICP-MS analysis and median values calculated based on in-situ, high spatial resolution analyses measured by LA-ICP-MS. The comparison yields favorable results for the vast majority of the trace elements investigated here with the exception of several elements, such as Hf, Zr, Th, and U. These differences can be mainly attributed to the inhomogeneous distribution of accessory precursor minerals (e.g., zircon) present in the arkosic sand at ground zero. Laser ablation analysis of Si-rich Trinitite samples yields inaccurate Ga abundance determinations since these are systematically too high, and may be attributed to a plasma-based polyatomic interference involving  $^{29}\text{Si} + ^{40}\text{Ar}$ . As noted in previous Trinitite investigations, Ca-rich areas are characterized by higher contents of Pu, and define a bomb-like signature  $^{240}\text{Pu}/^{239}\text{Pu}$  ratio ( $\sim 0.022$ ). Overall, the comparative results reported here confirm the effective and valid use of the LA-ICP-MS technique for deciphering the chemical and isotopic signatures of the nuclear device in post-detonation materials, and is therefore a valuable tool in nuclear forensic applications for source attribution purposes.

## Acknowledgments

We thank Sandy Dillard, Brazos Valley Petrographic Thin Section Services Lab (Bryan, TX) for production of high quality thin sections. The Center of Environmental Science and Technology (CEST) at the University of Notre Dame is thanked for the training and use of the  $\mu$ -XRF. Comments from two anonymous reviewers are greatly appreciated and have resulted in an improved version of the manuscript.

## Conflict of Interest

The authors report there are no conflicts of interest.

## Funding

This work was supported by DOE/NNSA (grant number PDPI11-40/DE-NA0001112).

## Supplemental Material

All supplemental material mentioned in the text, including three figures and four tables, is available in the online version of the journal, at <http://asp.sagepub.com/supplemental>.

## References

- I.D. Hutcheon, M.J. Kristo, K.B. Knight. "Nonproliferation Nuclear Forensics". In: P.C. Burns, G.E. Simon, editors. *Uranium: Cradle to Grave*. Mineralogical Association of Canada, 2013. pp. 377–394.
- P.P. Parekh, T.M. Semkow, M.A. Torres, D.K. Haines, J.M. Cooper, P.M. Rosenberg, M.E. Kitto. "Radioactivity in Trinitite Six Decades Later". *J. Environ. Radioact.* 2006. 85: 103–120.
- N. Eby, R. Hermes, N. Charnley, J.A. Smoliga. "Trinitite: The Atomic Rock". *Geol. Today*. 2010. 26(5): 180–185.
- A.J. Fahey, C.J. Zeissler, D.E. Newbury, J. Davis, R.M. Lindstrom. "Post-detonation Nuclear Debris for Attribution". *Proc. Natl. Acad. Sci. U.S.A.* 2010. 107(47): 20207–20212.
- J.J. Bellucci, A. Simonetti, C. Wallace, E.C. Koeman, P.C. Burns. "Isotopic Fingerprinting of the World's First Nuclear Device Using Post-Detonation Materials". *Anal. Chem.* 2013. 85: 4195–4198.
- J.J. Bellucci, A. Simonetti, C. Wallace, E.C. Koeman, P.C. Burns. "The Pb Isotopic Composition of Trinitite Melt Glass: Evidence for the Presence of Canadian Industrial Pb in the First Atomic Weapon Test". *Anal. Chem.* 2013. 85: 7588–7593.
- C. Wallace, J.J. Bellucci, A. Simonetti, T. Hainley, E.C. Koeman, P.C. Burns. "A Multi-Method Approach for Determination of Radionuclide Distribution in Trinitite". *J. Radioanal. Nucl. Chem.* 2013. 298: 993–1003.
- J.J. Bellucci, A. Simonetti, E.C. Koeman, C. Wallace, P.C. Burns. "A Detailed Geochemical Investigation of Post Nuclear Detonation Trinitite Glass at High Spatial Resolution: Delineating Anthropogenic vs. Natural Components". *Chem. Geol.* 2014. 365: 69–86.
- E.C. Koeman, A. Simonetti, P.C. Burns. "Sourcing of Copper and Lead within Red Inclusions from Trinitite Post-Detonation Material". *Anal. Chem.* 2015. 87: 5380–5386.
- J.J. Bellucci, A. Simonetti. "Nuclear Forensics: Searching for Nuclear Device Debris in Trinitite-hosted Inclusions". *J. Radioanal. Nucl. Chem.* 2012. 293: 313–319.
- P.H. Donohue, A. Simonetti, E.C. Koeman, S. Mana, P.C. Burns. "Nuclear Forensic Applications Involving High Spatial Resolution Analysis of Trinitite Cross-Sections". *J. Radioanal. Nucl. Chem.* 2015. 306: 457–467.
- J.J. Bellucci, C. Wallace, E.C. Koeman, A. Simonetti, P.C. Burns, J. Kieser, E. Port, T. Walczak. "Distribution and Behavior of Some Radionuclides in the Trinity Nuclear Test". *J. Radioanal. Nucl. Chem.* 2013. 29: 2049–2057.
- E. Van Achterbergh, C.G. Ryan, S.E. Jackson, W. Griffin. "Data Reduction Software for LA-ICP-MS". In: P. Sylvester, editor. *Laser Ablation-ICPMS in the Earth Sciences: Principles and Applications*. Mineralogical Association of Canada, 2001. pp. 239–243.
- G.A. Jenner, H.P. Longerich, S.E. Jackson, B.J. Fryer. "ICP-MS – a Powerful Tool for High-Precision Trace-Element Analysis in Earth Sciences: Evidence from Analysis of Selected U.S.G.S. Reference Samples." *Chem. Geol.* 1990. 83: 133–148.
- F.J. Pettijohn. "The Chemical Composition of Sandstones—Excluding Carbonate and Volcanic Sands". In: M. Fleischer (ed.) *Data of Geochemistry*, 6th ed. Washington: U.S. Geological Survey Professional Paper, 1963, pp.1–21Chap. 5.
- R.L. Rudnick, S. Gao. "Composition of the Continental Crust". In: R.L. Rudnick (ed.) *The Crust*. Vol. 3, Kidlington, UK: Elsevier, 2003, pp.1–64.
- R.L. Douglas. "Levels and Distribution of Environmental Plutonium Around the Trinity Site". ORP/LV-78-3: U.S. Environmental Protection Agency, Office of Radiation Programs, Las Vegas Facility, Las Vegas, Nevada, October (1978).